What to Do When the F10.7 Goes Out?

Elvidge, Sean; Themens, David R.; Brown, Matthew K.; Donegan-Lawley, Elizabeth

DOI:
10.1029/2022SW003392

Document Version
Publisher's PDF, also known as Version of record

Citation for published version (Harvard):
Elvidge, S, Themens, DR, Brown, MK & Donegan-Lawley, E 2023, 'What to Do When the F10.7 Goes Out?', *Space Weather*, vol. 21, no. 4, e2022SW003392. https://doi.org/10.1029/2022SW003392

Space Weather

RESEARCH ARTICLE
10.1029/2022SW003392

What to Do When the F10.7 Goes Out?

Sean Elvidge[1], David R. Themens[1], Matthew K. Brown[1], and Elizabeth Donegan-Lawley[1]

[1]Space Environment and Radio Engineering Group (SERENE), University of Birmingham, Birmingham, UK

Key Points:

- The F10.7 index is a critical value used in modeling of the upper atmosphere
- If the index is unavailable the closest way to reconstruct it is by using solar radio fluxes at other wavelengths
- Sunspot number can also be used to reconstruct F10.7 but rotation, running means, or constant values do not provide good approximations

Correspondence to:

S. Elvidge,
s.elvidge@bham.ac.uk

Citation:

Elvidge, S., Themens, D. R., Brown, M. K., & Donegan-Lawley, E. (2023). What to do when the F10.7 goes out? *Space Weather*, *21*, e2022SW003392. https://doi.org/10.1029/2022SW003392

Received 14 DEC 2022
Accepted 20 MAR 2023

Abstract The solar radio flux at 10.7 cm, known as F10.7, is a critical operational space weather index. However, without a clear backup, any interruption to the service can result in substantial errors in model outputs. In this paper we show the impact of one such outage in March 2022 on the models TIE-GCM and NeQuick, and present a number of alternative solutions that could be used for future outages. The analysis is extended to the F10.7 time series since 1951 and the approach resulting in the smallest reconstruction error of F10.7 uses the solar radio flux observations at alternative wavelengths (the best giving a percentage error of 3.1%). Alternatively, use of Sunspot Number, a regular, robust alternative observation, results in a mean percentage error of 8.2% and is also a reliable fallback solution. Additionally, analysis of the error on the use of the conversion between the 12-month rolling sunspot number (R12) and its conversion to F10.7 is included.

Plain Language Summary Models of the upper atmosphere rely on a variety of indices and drivers to run; one of the most common is a measurement of the 10.7 cm radio wavelength flux from the Sun, known as the F10.7. It has been continuously measured in Canada since 1947, and this long record makes it an excellent index for investigating upper atmosphere variations over a wide range of timescales. However, even though the index is used operationally at many space weather centres, there are currently no backup or alternative direct observations of F10.7. This paper describes a number of alternative observations which can be used to "fill in" for the F10.7 should there be a break in the observations, as there was in March 2022.

1. Introduction

The solar radio flux at 10.7 cm, known as F10.7, is one of the most commonly used indices of solar activity. It is used to drive both statistical and first principles models of the ionosphere and thermosphere and finds use in a wide range of applications spanning radio communications and navigation modeling (e.g., Warrington et al., 2009; ITU-R P.2297-0, 2013; Datta-Barua et al., 2014; Themens et al., 2021), remote sensing (e.g., Yeo et al., 2015; Ruck & Themens, 2021; Thomas & Shepherd 2022), solar physics (e.g., Tapping & Morgan, 2017; Brooks et al., 2017), and space environment climate and modeling (Matthes et al., 2017; Chapman et al., 2018; Kodikara et al., 2018; Elvidge & Angling, 2019; Nugent et al., 2020; Bilitza et al., 2022). F10.7 is used as a proxy for the solar extreme ultraviolet (EUV) forcing of the upper atmosphere and has been measured since 1947 (K. F. Tapping, 2013). Each reported F10.7 value is a ground observation of the total radio emission in a 100 MHz-wide channel centered at 2,800 MHz (wavelength of 10.7 cm) from all sources on the solar disk. The observations can be made from the ground since this wavelength does not ionize or heat the atmosphere. Three of these flux density observations are made each day, at 17:00, 20:00, and 23:00 UT (except during winter when the times are 18:00, 20:00, and 22:00 UT). The observation is expressed in solar flux units (sfu), where $1\,\text{sfu} = 10^{-22}\ \text{Wm}^{-2}\,\text{s}$.

The use of F10.7 in such a broad range of models, from research to operations, can at least partially be ascribed to the fact that it is a stable, long-term, ground-based observation that has been used to investigate variations over a wide range of timescales (Dudok de Wit & Bruinsma, 2017). From 1947 to 1991 the F10.7 was measured in Ottawa, Canada when the site was moved to the Dominion Radio Astrophysical Observatory (DRAO) in Penticton, Canada. The DRAO, which provides the F10.7 data freely to the community, is supported by the National Research Council of Canada in partnership with Natural Resources Canada (NRCan). This data stream is used globally for operational space weather products including those from the US Space Weather Prediction Center and the UK Met Office Space Weather Operations Centre. Thus, it is critical for operational space environment monitoring, forecasting, and mitigation services. However, this critical reliance of a wide variety of operational systems on a steady stream of F10.7 measurements poses a risk to the performance of these systems, should the F10.7 data stream be interrupted, particularly if such an interruption lasts more than a few days.

Such an interruption occurred on 18 March 2022, when a cyberattack caused a network interruption at the NRC, which resulted in an F10.7 outage that lasted over a month. Without redundant systems, many critical space weather architectures suddenly become unavailable, or, perhaps worse, generate output using "default values" of F10.7 (e.g., an F10.7 of 100 sfu) which can also be used for forcings in forecasts, potentially producing substantial errors without suitable warnings. For example, both the International Reference Ionosphere (Bilitza et al., 2022) and the Empirical Canadian High Arctic Ionospheric Model (Themens et al., 2017) immediately revert to the use of NOAA long-term F10.7 forecasts if measured values are not available. On 18 March 2022, resorting to these forecasts constituted an immediate error of ∼14 sfu, increasing to an error of ∼70 sfu just 10 days later as an active region rotated onto the disk.

In this study we explore the impacts of having to mitigate the F10.7 interruption experienced in March 2022 using a number of methods and investigate their suitability as an F10.7 redundancy.

2. Models

In addition to DRAO in Canada, the other notable observatory which records solar radio flux is the Nobeyama Radio Observatory in Japan (previously recorded in Toyokawa from 1951 to 1994), operated by the National Astronomical Observatory of Japan (https://solar.nro.nao.ac.jp/norp/), which makes continuous observations of flux densities at wavelengths of 30, 15, 8, and 3.2 cm (Tanaka et al., 1973). The 30 cm flux (from herein called F30) can be used by the Drag Temperature Model (DTM) and Dudok de Wit and Bruinsma (2017) argue that it is more sensitive than the 10.7 cm flux to longer wavelengths in the UV. Whilst the Nobeyama observatory does not observe the F10.7 flux density, which many space weather models require, the wavelengths measured can be used to generate a proxy for F10.7. A simple expression using just the observation at 15 cm (from herein called F15), which is the observation best correlated with the F10.7, can be found using non-linear least squares to low-order polynomials. For example, by fitting all available data, spanning November 1951 to November 2022, to a second-order polynomial, we find the following expression for adjusted F10.7 using F15:

$$\mathrm{F10.7}_{F15} = 0.00093 \cdot \mathrm{F15}^2 + 0.97 \cdot \mathrm{F15} + 15.43. \tag{1}$$

This results in an average root mean square error, compared to the measured F10.7, of ∼7 sfu. This can be further reduced to ∼6 sfu using a more complicated expression that also incorporates F8 (solar flux at 8 cm wavelength):

$$\mathrm{F10.7}_{F15F8} = 0.00054 \cdot \mathrm{F15}^2 + 0.25 \cdot \mathrm{F15} - 0.0012 \cdot \mathrm{F8}^2 + 0.85 \cdot \mathrm{F8} + 0.0012 \cdot \mathrm{F15} \cdot \mathrm{F8} - 8.67. \tag{2}$$

Both expressions enable a value of F10.7 to be used in case of an outage at the Penticton observatory, using observations from Nobeyama.

Additionally, the Collecte Localisation Satellites (CLS) group in France provide a routinely updated file (https://spaceweather.cls.fr/services/radioflux/) of both the absolute observations and 1 AU corrected observations of F3.2, F8, F15, and F30. This file also contains the observed and interpolated values of F10.7, where an (undescribed) method is used to fill in missing or poor quality F10.7 flux data using measurements at the other solar flux wavelengths. It should be noted that since 1 May 2018, the F10.7 in the CLS database is entirely composed of interpolated values rather than measurements since they gather their F10.7 from the no longer supported NOAA repository which was last updated in May 2018.

More commonly used approaches to estimate F10.7, rather than using additional solar radio flux wavelengths, concern the sunspot number (SN) (Clette, 2021). Historically, a wide range of formulae have been used to describe the relationship between F10.7 and SN. Tables 1 and 2 in Clette (2021) describe 18 such formulae, based on either version 1 (SN_{v1}) or version 2 (SN_{v2}) of the Sunspot Number (Clette & Lefèvre, 2016; Clette et al., 2014). Clette (2021) also describes a new high-degree polynomial fit using SN_{v2} given by:

$$\mathrm{F10.7}_{Clette} = 1.225 \times 10^{-8}\mathrm{SN}_{v2}^4 - 1.033 \times 10^{-5}\mathrm{SN}_{v2}^3 + 2.613 \times 10^{-3}\mathrm{SN}_{v2}^2 + 0.3938\mathrm{SN}_{v2} + 69.41. \tag{3}$$

One equation that was not presented in Clette (2021), which uses the 12-month running SN_{v1} ($\mathrm{R12}_{v1}$), is perhaps the most commonly used equation amongst all of them:

$$\mathrm{F10.7}_{R12_{v1}} = 0.00089 \cdot \mathrm{R12}_{v1}^2 + 0.728 \cdot \mathrm{R12}_{v1} + 63.7. \tag{4}$$

This equation is used in both the International Reference Ionosphere (IRI) model (Bilitza et al., 2017) and NeQuick (Nava et al., 2008), as well as in a variety of other places. However, seemingly like the child's game "Telephone" a key term is often missing from Equation 4, $F10.7_{12}$. The equation was designed as a relationship between R12 and the 12-month running mean of F10.7, $F10.7_{12}$ (now more commonly referred to as $F10.7_{365}$; the 365-day running mean) not as a relationship to F10.7 directly (Bilitza, 1990). When using the 12-month running mean of F10.7 the equation is part of the ITU-R Recommendation (ITU-R P.371-8, 1999). This misuse may be in part explained by the fact that the relationship in Equation 4 provides a slightly better fit (smaller standard deviation of errors) to the daily F10.7 than the equation specifically designed for that purpose ($F10.7_{CCIR} = 23e^{-0.05R12_{v1}} + R12_{v1} + 46$) also given in Bilitza (1990).

It is important to note that Equation 4, is still used by the IRI and NeQuick, but must use SN_{v1} since the internal empirical relationships were developed with that version of the SN. However, SN_{v1} is no longer produced and the recorded values must be "converted" back to version 1. This should be done using the ratio

$$SN_{v2} = \frac{SN_{v1}}{0.6 \times 1.177} = \frac{SN_{v1}}{0.7062}, \quad (5)$$

where the 0.6 is due to the change of reference observer and the 1.177 is to offset an inflation factor in the original SN values since 1946 (Clette, 2021). The relationship between SN_{v2} and SN_{v1} is roughly linear, and more complex expressions do not significantly reduce the root mean square error (RMSE) between the version 2 and version 1 conversion of approximately 6.2 sunspots.

The use of Equation 4 is not a problem in NeQuick as users input an F10.7 value that is then converted to $R12_{v1}$; however in the IRI, both F10.7 and $R12_{v1}$ are required by various submodules (e.g., F10.7 used by Danilov et al. (1995), Shubin (2015), Fejer et al. (2008) and $R12_{v2}$ by Altadill et al. (2013) and Scotto et al. (1997) [for a complete list see Table 8 of Bilitza et al. (2022)]). Returning to our previous example of the behavior of the IRI during the March 2022 F10.7 interruption, one could attempt to mitigate the errors caused by the reversion to the NOAA F10.7 forecast by applying one of the many relationships above to determine a synthetic F10.7 that could be manually inputted with the model call. If the IRI is run with no specified options it will use $R12_{v2}$, F10.7, the 81-day centered-mean of F10.7 (Richards et al., 2006) from its internal databases, convert $R12_{v2}$ to $R12_{v1}$ using Equation 5, and run the model. The 81-day mean F10.7 is used since the average of it with F10.7, $PF10.7 = (F10.7 + F10.7_{81})/2$, correlates well with changes in EUV (Richards et al., 2006). However users can directly specify the daily and 81-day mean F10.7 and/or $R12_{v2}$. If only one is provided then the other is calculated using Equations 4 and 5 (although noting that the IRI uses a value of 0.7 instead of 0.7062). This enables the IRI to mitigate against an F10.7 interruption through the use of $R12_{v2}$; however, this approach results in a mean absolute percentage error of 14.3% in specification of the F10.7, which is then used in the model; users should eliminate this error when driving the IRI with user inputs by passing both the $R12_{v2}$ and F10.7. However, users of IRI cannot manually provide $F10.7_{365}$ and the daily or 81-day value is used in its place and Equation 4 is assumed to hold for them. This is particularly problematic in the IRI if using "older" Sub-Models which require $F10.7_{365}$ such as that for the E-peak specification (Kouris & Muggleton, 1973) or ion composition (Danilov & Smirnova, 1995; Danilov & Yaichnikov, 1985). During an F10.7 outage, other methods, as we will show in the following section, can provide much greater performance than relying on the simple internal relationship to $R12_{v2}$.

3. Results

During the outage, the observed F10.7 changed by over 50 flux units, an increase of more than 60%. To put this in context, the mean percentage change over a 30-day period is 31% (albeit with a standard deviation of 19%), meaning that the outage period in question is ~1.5 standard deviations above the average variation that we would expect over such a period. To investigate the impact the replacements for F10.7 in upper atmosphere models, the Thermosphere Ionosphere Electrodynamics General Circulation Model (TIE-GCM; (Qian et al., 2014)) and NeQuick (Nava et al., 2008) has been driven with the observed F10.7 (adjusted to correct for the changing distance between the Earth and the Sun) until the outage on 18 March 2022, at which point each of the above F10.7 models have been used for the remaining runs of TIE-GCM and NeQuick. All other parameters are kept the same. TIE-GCM was run at 5° resolution, with a 30s model timestep and using the observed Kp. These have then been compared to a "true" run using the observed F10.7 values after the outage was fixed. The F10.7 replacement models are:

1. F15—The F10.7 derived from the 15 cm flux, Equation 1
2. F15 and F8—The F10.7 derived from the 15 and 8 cm flux, Equation 2

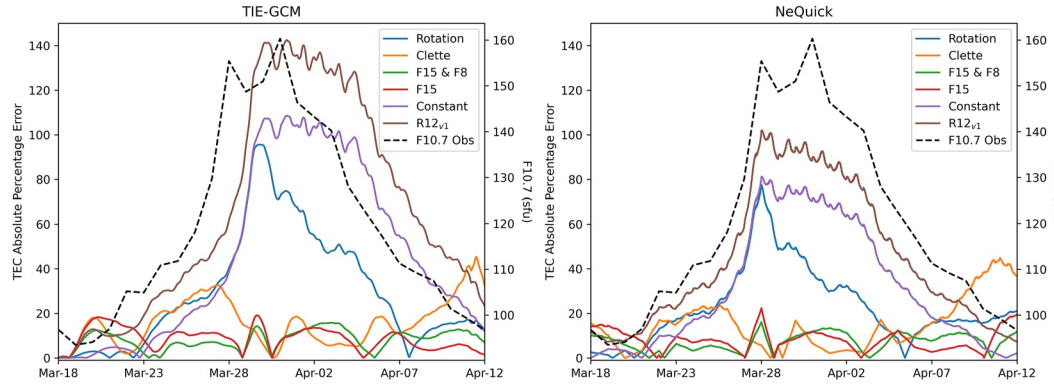

Figure 1. Absolute percentage error of total electron content (TEC) across the F10.7 outage time period in March and April 2022 for TIE-GCM (left) and NeQuick (right).

3. Clette—The updated fourth-order polynomial estimating F10.7 from the daily SN_{v2}, Equation 3
4. $R12_{v1}$—The ITU-R recommendation for estimating F10.7 from $R12_{v1}$ as used by, amongst others, the IRI, Equation 4
5. Constant—The F10.7 is held at a constant value of 97.8 throughout the model run, the last observation before the outage started
6. 27-Day Rotation—The value from 27 days ago is assumed as the current value

Figure 1 shows the global mean, absolute percentage error of the total electron content (TEC) in the ionosphere for the six different F10.7 replacement models, as previously described. Absolute percentage error (APE) is defined as:

$$\mathrm{APE} = \left| \frac{\mathrm{observation}_i - \mathrm{truth}_i}{\mathrm{truth}_i} \right| \times 100 \tag{6}$$

for an observation and truth time series of length N. It is clear, and unsurprising, that the models based on closely-related other observation data, F15, F15, and F8 and Clette, do significantly better than the model based on $R12_{v1}$, a constant value and the rotation model for both TIE-GCM and NeQuick. Note that TEC is usually defined as the path integral of electron density from ground to GNSS altitudes (~20,000 km), however TIE-GCM only provides output to 500–700 km (depending on solar conditions; in this case the model lid is ~615 km), and so the presented TECs are integrated from ground to 615 km for both TIE-GCM and NeQuick.

Overall both TIE-GCM and NeQuick respond very similarly to the different F10.7 models, with the TIE-GCM absolute percentage errors slightly larger than NeQuick. The largest error, from the $R12_{v1}$ method, is approximately 140% for TIE-GCM and 100% for NeQuick. For NeQuick the response in the model is immediate with changes in F10.7, for example, between March 24 and 28. However the TIE-GCM response to changes in F10.7 is delayed, by approximately 24–36 hr (Vaishnav, Jacobi, et al., 2021; Vaishnav, Schmölter, et al., 2021). Across the whole time period the model that uses either F15 alone (Equation 1) or both F15 and F8 (Equation 2) performs the best, slightly outperforming the Clette model at the beginning and end of the time period (with a similar performance between all three in the middle of the test period).

In contrast to Figure 1, which shows the overall global absolute percentage error in TEC, Figure 2 gives an example of the global TEC differences in TIE-GCM on March 27 at 1000, nine days after the outage began. It is still clear that the $R12_{v1}$, Constant, and Rotation models give the largest errors, and all of the models have the largest errors around the equatorial anomaly, where TEC values are typically largest.

The results presented thus far only cover the specific outage period from March and April 2022. To perform a more rigorous study of the different approaches, the error statistics of the different F10.7 proxy models have been compared to the observed F10.7 over a 71-year period (from November 1951 to November 2022). In replacement of the "Constant" model used previously an additional model, the average F10.7 across the 71-year time interval (120 sfu) has been used.

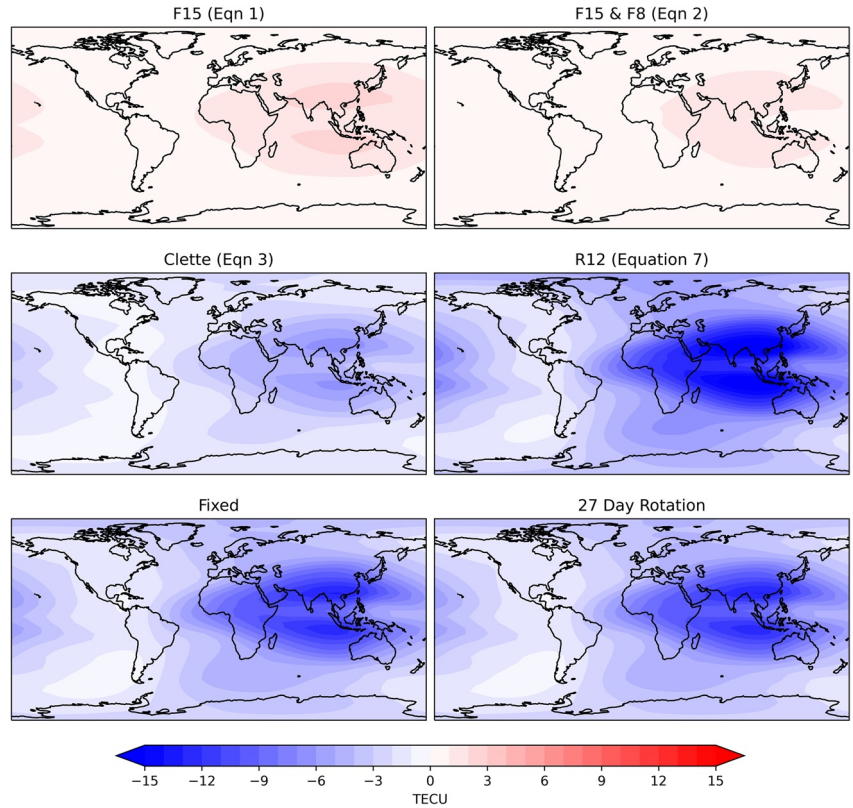

Figure 2. Error in total electron content (TEC) in TIE-GCM between using the observed F10.7 and the different F10.7 models at 1000 on 27 March.

The overall error statistics shown in Table 1 are in line with the previous example, the models using additional solar flux observations at 15 cm (F15) and 8 cm (F8) wavelengths, and F15 alone, perform best, with a mean absolute percentage error of 3.13% and 3.73% respectively. The Clette model also performs very well with ~8% error, followed by the Rotation, $R12_{v1}$ and the worse performing model (unsurprisingly) is the Average F10.7 model with a 38.5% error. Figure 3 shows a scatter plot comparing the five methods (excluding the "Average F10.7" model), overall each of the models have a strong linear correlation with the observations, with the $R12_{v1}$ model performing worst and the F15 and F8 model the best.

Table 1
Error Statistics of Different Models for Estimating F10.7

Model	Mean absolute percentage error (%)	Bias (sfu)	RMSE (sfu)	Correlation
F15 (Equation 1)	3.73	0.25	7.12	0.991
F15 and F8 (Equation 2)	3.13	0.73	6.00	0.994
Clette (Equation 3)	8.18	−0.13	15.3	0.956
$R12_{v1}$ (Equation 4)	13.9	−1.46	26.7	0.864
Average F10.7 (120 sfu)	38.5	−0.02	52.1	-
27-Day Rotation	11.6	−0.03	24.9	0.886

4. Conclusions

The solar radio flux at 10.7 cm, F10.7, is a critical index for space weather modeling and is one of the most commonly applied indices of solar activity used to drive both statistical and first principles models of the ionosphere and thermosphere. A number of operational systems rely on the F10.7; as such, a serious risk is posed by an interruption to the F10.7 data stream. Such an interruption occurred on 18 March 2022 when the F10.7 observations could not be made available due to a cyberattack. Without any clear, redundant system, models can stop working or can rely on default values (often without providing suitable warnings).

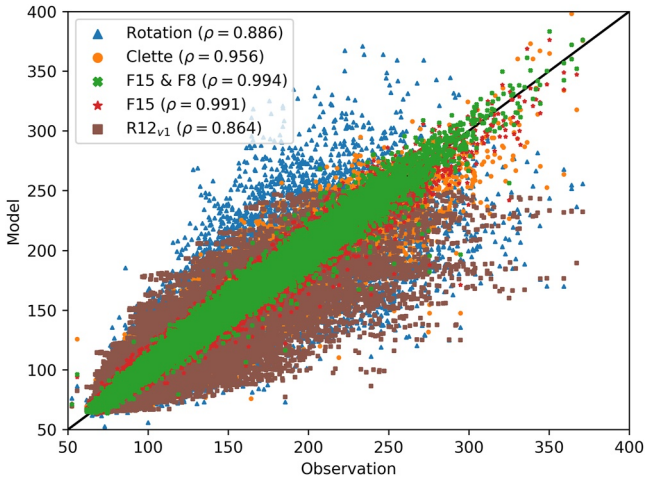

Figure 3. Scatter plot comparing five different methods, all show a strong positive correlation with the observed F10.7, but with the F15 and F8 (Equation 2) and F15 (Equation 1) perform best with correlations of 0.994 and 0.991 respectively.

This paper has presented a number of proxy models for F10.7, based on flux densities at 15 and 8 cm, sunspot number, 12-month mean sunspot number, 27-day rotations and using a fixed value. The impact of the these different F10.7 proxy models on the physics-based upper atmosphere model TIE-GCM and the empirical NeQuick has been demonstrated. It has been shown using historic F10.7 observations since 1951 that the use of the average F10.7, 12-month mean sunspot number and the 27-day rotation in proxy models causes significant errors in estimating F10.7 (38.5%, 13.9%, and 11.6% respectively, in terms of absolute percentage error) and should be avoided in an operational setting if there is a loss of F10.7. The best performing proxy models rely on using additional wavelength observations at 15 and 8 cm, which can be used to reconstruct F10.7 with just a 3.1% error. Using the best fitting high-order polynomial fit of sunspot number (SN_{v2}) to F10.7, as described by Clette (2021), results in an 8.2% error. Whilst this approach clearly performs worse, it has the advantage of being based on a robust observation, with recorded daily observations from 1818, making it a good choice as a redundant option for operational systems or in the backwards reconstruction of F10.7 for events prior to 1947.

Data Availability Statement

The F10.7 observations are recorded at the Dominion Radio Astrophysical Observatory, and freely provided to the space weather community with support from Natural Resources Canada. We are immensely grateful to them for their continued effort in providing this critical resource. The data daily and monthly and rotational averages can be downloaded from https://spaceweather.gc.ca/forecast-prevision/solar-solaire/solarflux/sx-5-en.php. The raw Nobeyama observations of F30, F15, F8 and F3.2 are available from https://solar.nro.nao.ac.jp/norp/data/daily/. Flare corrected, and Sun-Earth distance adjusted values are provided by Collecte Localisation Satellites (CLS) available from ftp://ftpsedr.cls.fr/pub/previsol/solarflux/observation/radio_flux_adjusted_observation.txt. Finally, the daily Sunspot Number is provided by WDC-SILSO, Royal Observatory of Belgium, Brussels, and can be downloaded from https://www.sidc.be/silso/DATA/EISN/EISN_current.csv.

Acknowledgments

SE and MKB are supported by the UK Space Weather Instrumentation, Measurement, Modelling and Risk (SWIMMR) Programme, National Environmental Research Council (NERC) Grants NE/V002643/1 and NE/V002708/1. DRT's contribution to this work is supported in part by DRivers and Impacts of Ionospheric Variability with EISCAT-3D (DRIIVE), NERC Grant NE/W003368/1.

References

Altadill, D., Magdaleno, S., Torta, J. M., & Blanch, E. (2013). Global empirical models of the density peak height and of the equivalent scale height for quiet conditions. *Advances in Space Research*, *52*(10), 1756–1769. https://doi.org/10.1016/j.asr.2012.11.018

Bilitza, D. (1990). *Solar-terrestrial models and application software*. National Space Sciences Data Center, World Data Center A for Rockets and Satellites, Goddard Space Flight Center.

Bilitza, D., Altadill, D., Truhlik, V., Shubin, V., Galkin, I., Reinisch, B., & Huang, X. (2017). International reference ionosphere 2016: From ionospheric climate to real-time weather predictions. *Space Weather*, *15*(2), 418–429. https://doi.org/10.1002/2016SW001593

Bilitza, D., Pezzopane, M., Truhlik, V., Altadill, D., Reinisch, B. W., & Pignalberi, A. (2022). The international reference ionosphere model: A review and description of an ionospheric benchmark. *Reviews of Geophysics*, *60*(4), e2022RG000792. https://doi.org/10.1029/2022RG000792

Brooks, D. H., Baker, D., van Driel-Gesztelyi, L., & Warren, H. P. (2017). A solar cycle correlation of coronal element abundances in Sun-as-a-star observations. *Nature Communications*, *8*(1), 183. https://doi.org/10.1038/s41467-017-00328-7

Chapman, S. C., Watkins, N. W., & Tindale, E. (2018). Reproducible aspects of the climate of space weather over the last five solar cycles. *Space Weather*, *16*(8), 1128–1142. https://doi.org/10.1029/2018SW001884

Clette, F. (2021). Is the F10.7cm – Sunspot number relation linear and stable? *Journal of Space Weather and Space Climate*, *11*, 2. https://doi.org/10.1051/swsc/2020071

Clette, F., & Lefèvre, L. (2016). The new sunspot number: Assembling all corrections. *Solar Physics*, *291*(9), 2629–2651. https://doi.org/10.1007/s11207-016-1014-y

Clette, F., Svalgaard, L., Vaquero, J. M., & Cliver, E. W. (2014). Revisiting the sunspot number. *Space Science Reviews*, *186*(1), 35–103. https://doi.org/10.1007/s11214-014-0074-2

Danilov, A. D., Rodevich, A. Y., & Smirnova, N. V. (1995). Problems with incorporating a new D-region model into the IRI. *Advances in Space Research*, *15*(2), 165–168. https://doi.org/10.1016/S0273-1177(99)80042-8

Danilov, A. D., & Smirnova, N. V. (1995). Improving the 75 to 300 km ion composition model of the IRI. *Advances in Space Research*, *15*(2), 171–177. https://doi.org/10.1016/S0273-1177(99)80044-1

Danilov, A. D., & Yaichnikov, A. P. (1985). A new model of the ion composition at 75 to 1000 km for IRI. *Advances in Space Research*, *5*(7), 75–79. https://doi.org/10.1016/0273-1177(85)90360-6

Datta-Barua, S., Walter, T., Bust, G. S., & Wanner, W. (2014). Effects of solar cycle 24 activity on WAAS navigation. *Space Weather*, *12*(1), 46–63. https://doi.org/10.1002/2013SW000982

Dudok de Wit, T., & Bruinsma, S. (2017). The 30 cm radio flux as a solar proxy for thermosphere density modelling. *Journal of Space Weather and Space Climate*, *7*(A9), A9. https://doi.org/10.1051/swsc/2017008

Elvidge, S., & Angling, M. J. (2019). Using the local ensemble Transform Kalman Filter for upper atmospheric modelling. *Journal of Space Weather and Space Climate*, *9*(A30), A30. https://doi.org/10.1051/swsc/2019018

Fejer, B. G., Jensen, J. W., & Su, S.-Y. (2008). Quiet time equatorial F region vertical plasma drift model derived from ROCSAT-1 observations. *Journal of Geophysical Research*, *113*(A5), A05304. https://doi.org/10.1029/2007JA012801

ITU-R P.2297-0. (2013). Electron density models and data for transionospheric radio propagation (P Series). Retrieved from https://extranet.itu.int/brdocsearch/R-REP/R-REP-P/R-REP-P.2297/R-REP-P.2297-2013/R-REP-P.2297-2013-MSW-E.docx

ITU-R P.371-8. (1999). ITU-R choice of indices for long-term ionospheric predictions, recommendation ITU-R P. 371-8. Retrieved from https://www.itu.int/dms_pubrec/itu-r/rec/p/R-REC-P.371-8-199907-I!!PDF-E.pdf

Kodikara, T., Carter, B., & Zhang, K. (2018). The first comparison between Swarm-C accelerometer-derived thermospheric densities and physical and empirical model estimates. *Journal of Geophysical Research: Space Physics*, *123*(6), 5068–5086. https://doi.org/10.1029/2017JA025118

Kouris, S. S., & Muggleton, L. M. (1973). A proposed prediction method for monthly median foE, contribution No. 6/03/07 to Interim Working Party 6/3 (No. CCIR Report 252-2).

Matthes, K., Funke, B., Andersson, M. E., Barnard, L., Beer, J., Charbonneau, P., et al. (2017). Solar forcing for CMIP6 (v3.2). *Geoscientific Model Development*, *10*(6), 2247–2302. https://doi.org/10.5194/gmd-10-2247-2017

Nava, B., Coisson, P., & Radicella, S. (2008). A new version of the neQuick ionosphere electron density model. *Journal of Atmospheric and Solar-Terrestrial Physics*, *70*(15), 1856–1862. https://doi.org/10.1016/j.jastp.2008.01.015

Nugent, L. D., Elvidge, S., & Angling, M. J. (2020). *Comparison of low-latitude ionospheric scintillation forecasting techniques using a physics-based model*. Space Weather.

Qian, L., Burns, A. G., Emery, B. A., Foster, B., Lu, G., Maute, A., et al. (2014). The NCAR TIE-GCM: A community model of the coupled thermosphere/ionosphere system. In J. Huba, R. Schunk, & G. Khazanov (Eds.), *Modeling the ionosphere-thermosphere system* (pp. 73–83). John Wiley & Sons, Ltd. https://doi.org/10.1002/9781118704417.ch7

Richards, P. G., Woods, T. N., & Peterson, W. K. (2006). HEUVAC: A new high resolution solar EUV proxy model. *Advances in Space Research*, *37*(2), 315–322. https://doi.org/10.1016/j.asr.2005.06.031

Ruck, J. J., & Themens, D. R. (2021). Impacts of auroral precipitation on HF propagation: A hypothetical over-the-horizon radar case study. *Space Weather*, *19*(12), e2021SW002901. https://doi.org/10.1029/2021SW002901

Scotto, C., Mosert de González, M., Radicella, S. M., & Zolesi, B. (1997). On the prediction of F1 ledge occurrence and critical frequency. *Advances in Space Research*, *20*(9), 1773–1775. https://doi.org/10.1016/S0273-1177(97)00589-9

Shubin, V. N. (2015). Global median model of the F2-layer peak height based on ionospheric radio-occultation and ground-based Digisonde observations. *Advances in Space Research*, *56*(5), 916–928. https://doi.org/10.1016/j.asr.2015.05.029

Tanaka, H., Castelli, J. P., Covington, A. E., Krüger, A., Landecker, T. L., & Tlamicha, A. (1973). Absolute calibration of solar radio flux density in the microwave region. *Solar Physics*, *29*(1), 243–262. https://doi.org/10.1007/BF00153452

Tapping, K., & Morgan, C. (2017). Changing relationships between sunspot number, total sunspot area and F10.7 in Cycles 23 and 24. *Solar Physics*, *292*(6), 73. https://doi.org/10.1007/s11207-017-1111-6

Tapping, K. F. (2013). The 10.7 cm solar radio flux (F10.7). *Space Weather*, *11*(7), 394–406. https://doi.org/10.1002/swe.20064

Themens, D. R., Jayachandran, P. T., Galkin, I., & Hall, C. (2017). The empirical canadian high arctic ionospheric model (E-CHAIM): NmF2 and hmF2. *Journal of Geophysical Research: Space Physics*, *122*(8), 9015–9031. https://doi.org/10.1002/2017JA024398

Themens, D. R., Reid, B., Jayachandran, P. T., Larson, B., Koustov, A. V., Elvidge, S., et al. (2021). E-CHAIM as a model of total electron content: Performance and diagnostics. *Space Weather*, *19*(11), e2021SW002872. https://doi.org/10.1029/2021SW002872

Thomas, E. G., & Shepherd, S. G. (2022). Virtual height characteristics of ionospheric and ground scatter observed by mid-latitude SuperDARN HF radars. *Radio Science*, *57*(6), e2022RS007429. https://doi.org/10.1029/2022RS007429

Vaishnav, R., Jacobi, C., Berdermann, J., Codrescu, M., & Schmölter, E. (2021). Role of eddy diffusion in the delayed ionospheric response to solar flux changes. *Annales Geophysicae*, *39*(4), 641–655. https://doi.org/10.5194/angeo-39-641-2021

Vaishnav, R., Schmölter, E., Jacobi, C., Berdermann, J., & Codrescu, M. (2021). Ionospheric response to solar extreme ultraviolet radiation variations: Comparison based on CTIPe model simulations and satellite measurements. *Annales Geophysicae*, *39*(2), 341–355. https://doi.org/10.5194/angeo-39-341-2021

Warrington, E. M., Bourdillon, A., Benito, E., Bianchi, C., Monilié, J.-P., Muriuki, M., et al. (2009). Aspects of HF radio propagation. *Annals of Geophysics*, *52*(3–4), 301–321. https://doi.org/10.4401/ag-4577

Yeo, K. L., Ball, W. T., Krivova, N. A., Solanki, S. K., Unruh, Y. C., & Morrill, J. (2015). UV solar irradiance in observations and the NRLSSI and SATIRE-S models. *Journal of Geophysical Research: Space Physics*, *120*(8), 6055–6070. https://doi.org/10.1002/2015JA021277